IEEE 802.11 WLANS: A COMPARISON ON INDOOR COVERAGE MODELS

Cassio Bento Andrade and Roger Pierre Fabris Hoefel

Department of Electrical Engineering - Federal University of Rio Grande do Sul (UFRGS)
Av. Oswaldo Aranha, 103 - Porto Alegre – RS - Brazil
cassio@cinted.ufrgs.br / roger.hoefel@ufrgs.br

***Abstract*— In this paper, it is used analytical and measurement tools in order to compare five different indoor path loss propagation models: one-slope; dual-slope; partitioned; Cost-231 multi-wall model and average walls. The main objective is to use the receive signal strength indicator (RSSI) in order to set a simple and fast procedure, taking into account accuracy, complexity and scalability, to estimate the coverage of IEEE 802.11 wireless local area networks (WLANs). We have concluded that the average walls model propitiate a better path loss prediction among the selected models.**

***Index Terms*—** *802.11, indoor path loss models, RSSI.*

I. INTRODUCTION

The Federal University of Rio Grande do Sul (UFRGS) in Brazil (www.ufrgs.br) has been working on a project of distance learning and digital inclusion that will be expanded in poor communities all over the country. To reach above goal, it is necessary to have a methodology to set up a wireless network attending the target coverage using a fast and simple procedure with inexpensive resources. Five indoor propagation models have been selected a priori: one-slope; dual-slope; partitioned; Cost-231 multi-wall model and average walls. The main objective of this contribution is to present a comparison, using numerical and field measurements, among the five selected propagation models to determine which is more suitable for this project implementation.

This paper is organized as follows. Section II briefly presents related works on indoor path loss prediction. Section III describes the five path loss indoor propagation models analyzed in this contribution. Section IV shows the measurement set up and the procedures used to determine the propagation model parameters. Section V carries out a comparison between numerical and measurement results, focusing on the tradeoffs between accuracy and complexity of the investigated propagation models. Section VI compares the site survey measurements with the results predicted by the numerical results. Finally, Section VII presents our final conclusions.

II. RELATED WORK

The classical one-slope propagation model [1-2], [3, p. 101] is a general path loss model that has been tested in a large number of environments, including industrial sites [4]. An improvement that offers a better accuracy is the dual-slope model [5]. Another model that has been used for residential, office and micro-cells is the partitioned model [3, p.104], [6].

The COST231 multi-wall model [7] has been widely used and it is a suitable model for initial WLAN planning in indoor environments, according to [8]. The average walls model has been proposed in [9] to minimize the design effort of WLANs.

III. PATH LOSS PROPAGATION MODELS

A. ONE-SLOPE MODEL

The path loss in dB is given by

$$L_{dB} = L_{0,dB} + 10n\log_{10} d. \quad (1)$$

where $L_{0,dB}$ is the path loss obtained at *1 meter* distant from the transmitter and the path loss exponent n is determined experimentally using an interpolation procedure [1].

B. DUAL-SLOPE MODEL

The path loss in dB is given by [4]

$$L_{dB} = L_{0,dB} + \begin{cases} 10n_1\log_{10} d, & 1m < d \le d_{bp} \\ 10n_1\log_{10} d_{bp} + 10n_2\log_{10}\left(\frac{d}{d_{bp}}\right), & d > d_{bp} \end{cases}, \quad (2)$$

where the path loss exponents n_1 and n_2 are determined experimentally. Basically, this model divides the distances into one line-of-sight (LOS) and one obstructed LOS region. The breakpoint distance d_{bp} takes into account that in indoor environments the ellipsoidal Fresnel zone can be obstructed by the ceiling or the walls, anticipating the LOS region:

$$d_{bp} = \frac{4h_b h_m}{\lambda}, \quad (3)$$

where h_b and h_m denote the shortest distance from the ground or wall of the access point (AP) and station (STA), respectively.

C. PARTITIONED MODEL

The path loss in dB is given by

$$L_{dB} = L_{0,dB} + \begin{cases} 20\log_{10} d\,, & 1m < d \le 10m \\ 20 + 30\log_{10}\left(\frac{d}{10}\right), & 10m < d \le 20m \\ 29 + 60\log_{10}\left(\frac{d}{20}\right), & 20m < d \le 40m \\ 47 + 120\log_{10}\left(\frac{d}{40}\right), & d > 40m \end{cases}. \quad (4)$$

This model uses pre-determined values for the path loss exponents and breakpoint distances, according to previous field measurement campaigns [3, p.104], [6].

D. COST 231 – MULTI-WALL MODEL

The path loss in dB is given by [7]

$$L_{dB} = L_{0,dB} + 20\log_{10} d + k_f^{\left[\frac{k_f+2}{k_f+1} - b\right]} L_f + \sum_{i=1}^{k_w} k_{wi} L_{wi}\,, \quad (5)$$

where k_f denotes the number of penetrated floors. The parameter b is used to fit empirically the non-linear effects of the number of floors on the path loss. L_f denotes the loss between adjacent floors. The integer k_w is the number of wall types; k_{wi} and L_{wi} denote the number and loss for walls of *ith* type, respectively.

The free-space path loss (FPL) in linear scale is given by

$$L_0 = \left(\frac{4\pi d_0}{\lambda}\right)^2, \quad (6)$$

where λ denotes the wavelength. For *2.4 GHz* Industrial, Scientific and Medical (ISM) band, λ=0.125 m, d_0=*1 m*, then the FPL in dB, $L_{o,dB}$, is equals to *40.2 dB*.

For practical reasons, the wall types are divided in only two categories, as shown in Tab. I.

Table I – Wall types for the multi-wall model.

Wall type	Description	Value [dB]
L_{w1}	Light wall: plasterboard, particle board or thin (<10 cm), light concrete wall.	3.4
L_{w2}	Heavy wall: thick (>10 cm), concrete or brick	6.9

E. Average Walls Model

This model is based on the Cost-231 multi-wall, excepted that the loss due to obstructing walls is aggregated in just one parameter L_w [9]. Therefore, for a single floor environment, the path loss estimated by (5) is modified to

$$L_{dB} = L_{0,dB} + 20log_{10}d + k_w L_w, \quad (7)$$

where k_w denotes the number of penetrated walls. In order to determine the parameter L_w, each wall obstructing the direct path between the receiver and the transmitter antennas must have its loss measured as follows.

The loss of the first wall in dB is given by:

$$L_1 = L - L_{0,dB} - 20log_{10}d, \quad (8)$$

where $L_{0,dB}$ is the path loss obtained at *1 meter* distant from the transmitter; L denotes the measured total loss from *1 meter* distant after the obstructing wall.

For the second wall the loss of the first wall also must be taken into account. Therefore, the loss in dB of the second obstructing wall can be estimated as

$$L_2 = L - L_{0,dB} - 20log_{10}d - L_1 . \quad (9)$$

Keeping on the above methodology, the *ith* wall loss is given by

$$L_i = L - L_{0,dB} - 20log_{10}d - \sum_{j=1}^{i-1} L_j , \quad (10)$$

where the sum spans the losses of walls obtained previously. After all wall losses of the environment had been obtained, then the wall losses average value is computed and assigned to the parameter L_w.

IV. Measurement Procedures

In order to exemplify the large set of field measurements that have been performed at UFRGS's laboratories, we selected a set of measurements at Multidisciplinary Center of New Technologies for Distance Education (CINTED). This laboratory uses an entire floor in a multi-floor building, as shown in Fig. 1. The walls are made of bricks, *15 cm wide*. This environment has two APs that presents a low (AP1) and high (AP2) occurrence of obstructing walls. The gray areas (the WC, kitchen and the staircase) are the only places that do not need network coverage.

The deployed network has two Linksys 802.11b/g APs, equipped with two dipole antennas each. A free test software *Netstumbler*, running on a notebook with an 802.11a/b/g card adapter, was used to perform the measurements. This simple approach allows determining a first order coverage procedure that can be applied in large scale (e.g. schools located in low income communities) with minimum human and material resources. The measurements have been performed using the following conventional notebook use: the AP's antenna is located at *90°* from the ground and the notebook is parallel to the ground, facing the AP's direction. The test software measures the received signal power level every second automatically. Twenty samples, with small displacements in order of the wavelength (λ = *0.125m*), are used to estimate the mean received power in dBm, $P_{rx,dB}$, at each selected point.

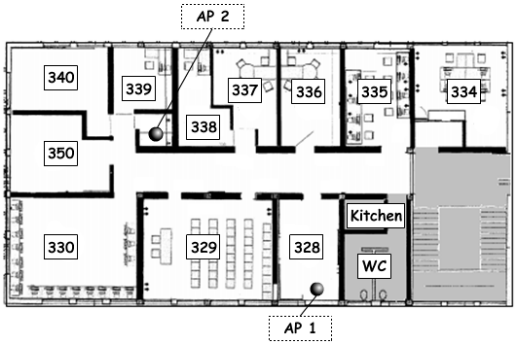

Fig. 1 – Coverage area and AP's location in CINTED.

The path loss for each distance is given by

$$L_{dB} = EIRP_{dBm} - P_{rx,dBm}, \quad (11)$$

where $EIRP_{dbm}$ denotes effective isotropic radiated power in dBm from the AP antenna. It is assumed that the notebooks have antennas with gain of 0 dBi.

To determine the parameters for the one-slope and dual-slope propagation models, the measurements were carried out for each *1 meter* distant from the AP of interest, as shown in Figs. 2a and 2b for the AP1 and AP 2, respectively. The data measured is plotted in a distance logarithmic scale and linear interpolation is used to obtain the parameters used in both models: the inclination determines the path loss exponent *n* and the intersection at distance of *1 meter* responds for the parameter $L_{0,dB}$.

To set up the parameters for the average walls model, it was just necessary to measure the average path loss for only one point located *1 meter* after each wall that obstructs the LOS path. Figs. 3a depicts the measurement points for AP1. For AP2 there is also one additional measure point for each wall (number 2 e 4) for accuracy improvement, as describe in Section V.

In order to parameterize the COST 231 model, then the brick walls are considered as heavy wall, as shown in Tab. I.

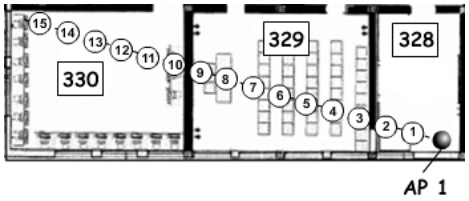

Fig. 2a – AP1.

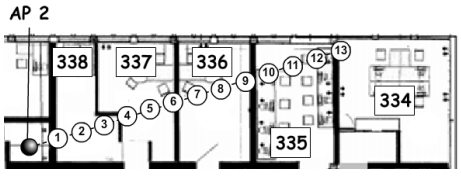

Fig. 2b – AP2.

Fig. 2 – Measure points to determine the parameters for one-slope and dual-slope propagation models.

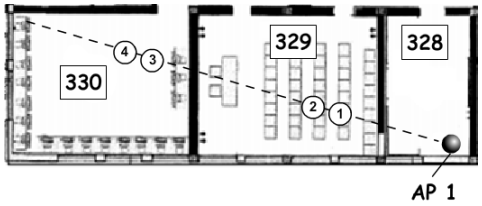

Fig. 3a – AP1.

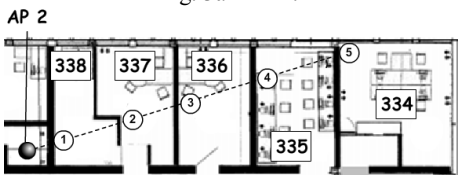

Fig. 3b – AP2.

Fig. 3 – Measure points for average walls propagation model.

V Numerical and Measurement Results

In this section, the measurement results are shown by geometric figures while the numerical ones are depicted as straight lines.

Figures 4a (AP1) and 4b (AP2) show results for the one-slope, dual-slope and partitioned path loss models. For AP 1 and AP 2, the one-slope model is given by (12) and (13), respectively, where it is used the parameterization procedure described in the previous section.

$$L_{dB} = 34.48 + 32.79log_{10}d. \quad (12)$$

$$L_{dB} = 48.58 + 18.67log_{10}d. \quad (13)$$

It is necessary to determine the breakpoint distance to set up the dual-slope model. For the AP 1, the closest distance between the ground, ceiling or walls is of *0.5 meters*; while for the AP 2 is of *0.65 meters*. The measurements were carried out at *0.5 meters* height. Hence, using (3), the distance breakpoint for AP1 and 2 are given by *8* and *10.4 meters*, respectively. Therefore, the dual-slope model for AP1 and AP2 is given by (14) and (15), respectively.

$$L_{dB} = 37.76 + \begin{cases} 27.15log_{10}d, & 1m < d \leq 8 \\ 24.52 + 42.79log_{10}\left(\frac{d}{8}\right), & d > 8 \end{cases}. \quad (14)$$

$$L_{dB} = 52.71 + \begin{cases} 11.38log_{10}d, & 1m < d \leq 10.4 \\ 11.57 + 65.67log_{10}\left(\frac{d}{10.4}\right), & d > 10.4 \end{cases}. \quad (15)$$

We can see, as expected, a noticeable attenuation due to obstructing walls (see the third measurement point in Figs 2a and 4a and the first, fourth, seventh, tenth and thirteenth measure points in Fig. 2b and 4b).

Comparing (12) with (14) and (13) with (15), we can verify that the parameter L_0 obtained in the one-slope model results in a lower value than the one obtained using the dual-slope model. Notice that as the first segment inclination in dual-slope model considers only measurements for the closest distances, then it takes a lesser path loss exponent value than the one obtained for one-slope estimation, that take into account the measurement results for all distances. These differences in the path loss exponent explain the different values for the parameter L_0.

Analyzing Fig. 4a, we conclude that the *dual slope model* allows slightly better path loss estimation in relation to the *one-slope model*. The *partitioned model* follows the measured results with a good accuracy in the first distance segment. However, the estimation curve diverges from the measured data after the breakpoint. For AP2, as shown in Fig. 4b, the *dual-slope model* presents again a better agreement with the measured data, mainly for the distances after the breakpoint. In this case, the *partitioned model* has not shown a good agreement in both segments, responding for the worst estimation of all the three models analyzed in this figure.

The maximum, the mean and the standard deviation error in dB between measured and numerical results for the one-slope, dual-slope and partitioned propagation models are shown in Tab. II.

Table II – Statistical errors between measured and estimation data for one-slope, dual-slope and partitioned propagation models.

Model	Maximum Error (dB)		Mean Error (dB)		Standard Deviation (dB)	
	AP 1	AP 2	AP 1	AP 2	AP 1	AP 2
One-Slope	4.64	9.22	2.29	3.91	1.45	2.99
Dual-Slope	5.28	7.61	2.05	2.85	1.77	1.87
Partitioned	11.01	15.17	6.15	7.16	3.12	4.25

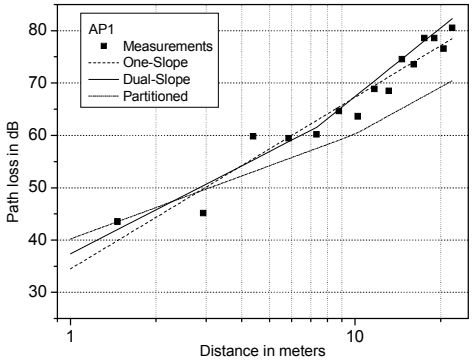

Fig. 4a – Access Point 1.

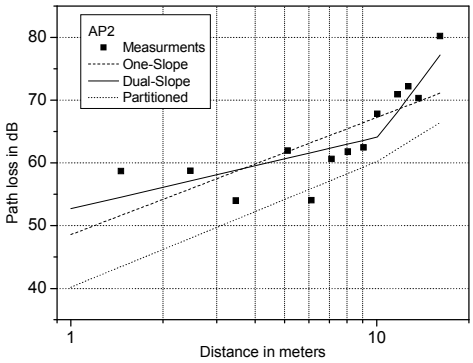

Fig. 4b – Access Point 2.

Fig. 4 - Measurement and numerical results for one-slope, dual-slope and partitioned propagation models.

Figures 5a (AP1) and 4b (AP2) show results for the dual-slope, COST 231 and average walls path loss models. The parameters for the COST 231 are: the brick walls with *15cm* width are considered as L_{W2} wall type, corresponding to *6.9 dB* attenuation for each obstructing wall for both AP1 and AP2. Hence, using (7), the path loss is given by

$$L_{dB} = 40.2 + 20log_{10}d + k_w \cdot 6.9. \quad (17)$$

For the *average walls model*, the aggregated wall loss L_w is experimentally determined according to item E of Section III. This procedure results in the data shown in Tab. III. We can verify a different attenuation among the walls due to the different surroundings. Even negative values are possible to be obtained (as in wall 2 for AP2 at Tab III), but the mean value always results in a

positive value.

Table III – Wall loss determination for average walls model.

Wall	AP 1	AP 2
1	3.90 dB	10.71 dB
2	8.62 dB	-12.60 dB
3		5.02 dB
4		6.76 dB
5		5.94 dB
Mean	6.26 dB	3.17 dB

Analyzing Fig 5a, we can see that the three models allow a good agreement with the data measured for AP 1. However, for AP 2, as shown in Fig 5b, the *COST 231 model* estimation diverges significantly from the measured data. Notice that the *average walls model* estimates a wall loss of 3.17dB (Tab. III) while it is used a loss 6.9 dB for COST 23 model (Tab. II).

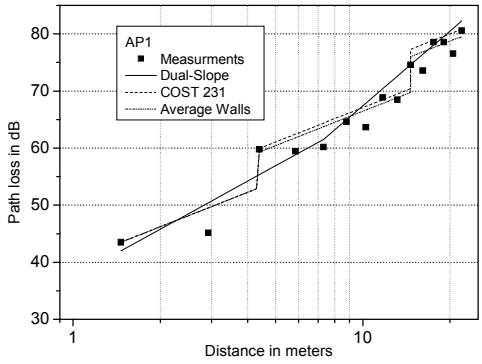

Fig. 5a – Access Point 1.

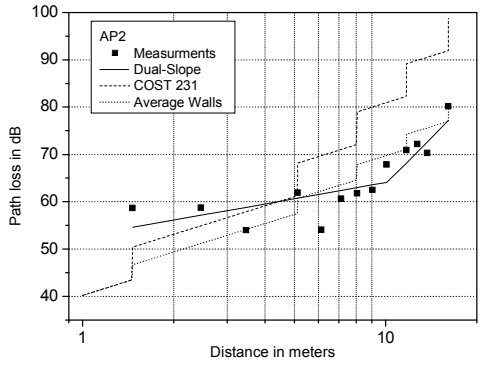

Fig. 5b – Access Point 2.

Fig. 5 - Measurement and numerical results dual-slope, COST 231 and average walls propagation models.

The maximum, the mean and the standard deviation errors between measured and numerical results for the *dual-slope*, *COST231* and *average walls models* are shown in Tab. IV. For AP 1, a better agreement is obtained by the average walls propagation model. However, for AP 2, this model does not present a good fitting in closer distances because the first wall presents a greater attenuation in relation to the obtained average value (see Tab III, wall 1 for AP 2). Although, the dual-slope model results in a better agreement for AP 2, this fact does not necessary mean a significant superiority over the average walls model accuracy. As shown in Tab. IV, the mean errors of differences between them are around only 2dB. We can infer that both models present a close accuracy. However, for practical reasons, the average walls model has a noticeable advantage: it requires lesser quantity of measurements for parameterization (2 measures against 15 from AP 1; 5 measures against 13 from AP 2).

Table IV — Statistical errors between measured and estimation data for dual-slope, COST 231 and average walls propagation models.

Model	Maximum Error (dB)		Mean Error (dB)		Standard Deviation (dB)	
	AP 1	AP 2	AP 1	AP 2	AP 1	AP 2
Dual-Slope	5.30	7.61	2.33	2.85	1.77	1.87
COST 231	4.58	20.25	2.05	12.70	1.74	5.93
Average Walls	4.34	12.00	1.63	4.82	1.38	3.53

VI. Site Survey

Figures 6a and 6b show the coverage map for AP 1 and AP 2, respectively, based on RSSI measurements.

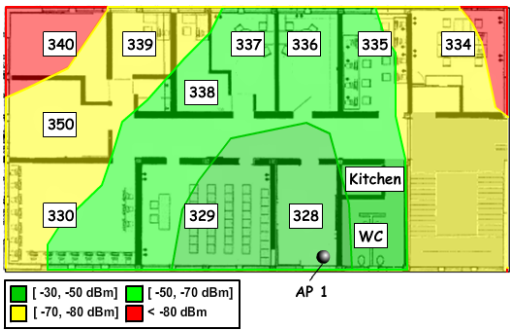

Fig. 6a –Access Point 1.

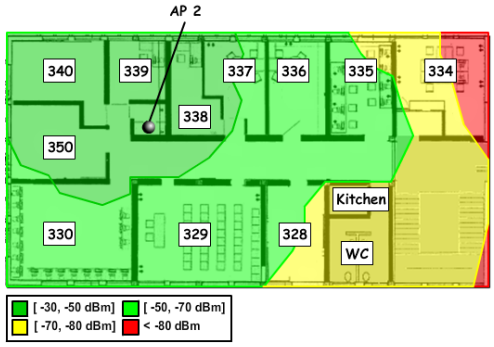

Fig. 6b –Access Point 2.

Fig. 6 – Coverage map obtained by the site survey.

Fig. 7a shows the estimated coverage map for the AP1 using the dual-slope propagation model. It is noticeable a good agreement (Fig. 7a) with measured data (Fig. 6a) for closer distances from the AP1. However, when the distances from de AP1 increases (the red area in rooms 334 and 340 at Fig 6a), the signal measured presents a greater attenuation than it is predicted by the model. This takes place due to a greater number of walls in relation to the environment where the parameters of model were obtained (see Fig. 2a).

Fig. 7b is analogous to Fig. 6b, except that it shows results for AP2. Here, opposite results are noticed. Since the parameterization was obtained in environment with a high occurrence of obstructing walls (see Fig. 2b), the model estimation presents a good agreement for farther distances form AP where it occurs a higher number of obstructing walls. However, in closer distances there is lesser

number of walls and the model predicts an overestimated loss in relation to the site survey measurements.

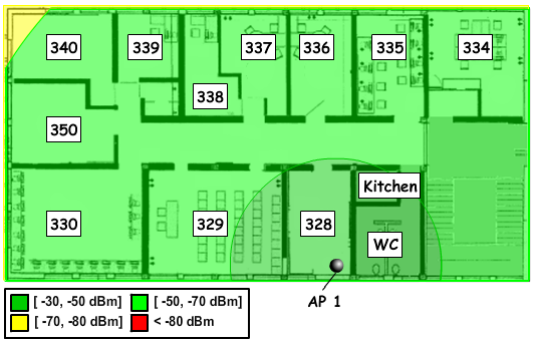

Fig. 7a –Access Point 1: dual-slope propagation model.

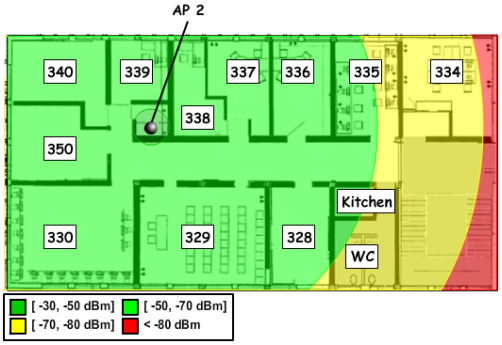

Fig. 7b – Access Point 2: dual-slope propagation model.

Fig. 7 – Estimated coverage map for dual-slope propagation model.

Fig. 8a shows the coverage map for the AP1 using the average walls propagation model. This modeling presents a good accuracy at closer distance for the AP 1 (like the dual-slope results shown in Fig. 6a) and a better agreement with the measured data at farther distances. Notice that the site survey (see Fig. 6a) shows attenuations below -80 dB at 334 and 340 rooms. These path losses are corrected predicted by the average walls model, as shown in Fig. 8a.

For AP 2, the estimations from average walls (Fig. 8a) and dual-slope (Fig. 7a) models are similar. However, none of the models predicted a larger attenuation in the bathroom walls, approximately 10dB. This phenomenon must be taken into account when planning the network as described in [9]. The walls next to WC present a greater attenuation than other building walls because inside them there are pipes embedded.

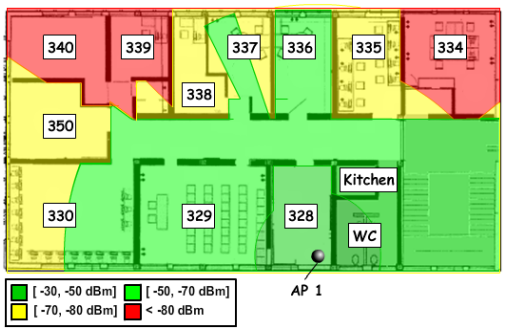

Fig. 8a –Access Point 1.

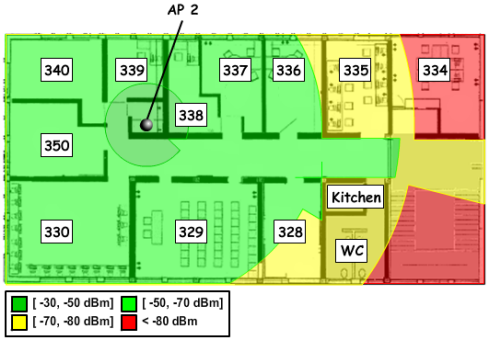

Fig. 8b –Access Point 2.

Fig. 8 – Estimated coverage map for average walls propagation model.

In the site survey procedure, shown in Fig. 6, a significant set of locations inside the building were chosen to calculate the errors between the numerical estimation and the site survey measurements. This procedure allows a fine comparison between the accuracy of the average walls and dual-slope models. Comparing Fig. 9a with Fig. 9b, we can that the average wall path loss model provides a lesser prediction in relation to the dual-slope model, mainly for farther distances from the access point. Figures 9c and 9d show results for AP 2. In this case, both models result in similar error values. These results ratify the remarks done in Tab. IV.

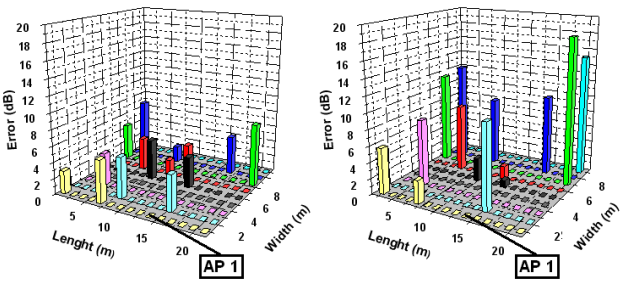

(a) Average walls model for AP1. (b) Dual Slope model for AP1.

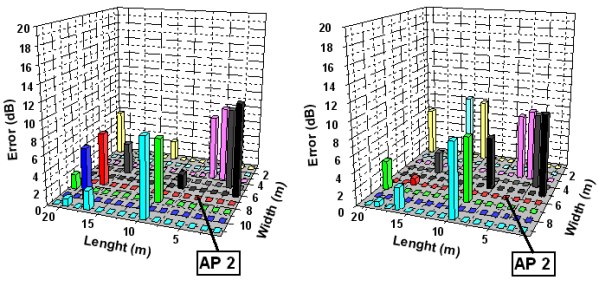

(a) Average walls model for AP2. (b) Dual Slope model for AP2.

Fig. 9 – Errors between received power between estimation and site survey measurement.

Finally, in order to compare the scalability of the average walls and dual-slope models, the predictions from them were tested in 25 locations where the users of that network would probably be. Tab V shows the maximum, mean and standard deviation errors between measured and estimated data. For both environments, we can see

that the average walls model provides a better estimation of the path loss, for the maximum and the mean error estimation. In addition to the mean error value complies with the shadowing margin, usually around of 8dB for IEEE 802.11 networks [10]. We can also verify that the average walls model provides a lesser standard deviation error. Finally, we claim that, although the dual-slope model presents a slightly better accuracy in a similar environment where the parameterization has been done for AP 2 (see Tab IV), the average walls model scalability has been proved to be superior.

Table V – Maximum, mean errors and standard deviation for dual-slope and average walls propagation models at 25 selected measured points.

Model	Maximum Error (dB)		Mean Error (dB)		Standard Deviation (dB)	
	AP 1	AP 2	AP 1	AP 2	AP 1	AP 2
Average Walls	6.40	22.73	2.67	7.52	2.56	6.84
Dual-Slope	16.26	25.31	6.41	9.25	4.73	7.89

VII. Conclusions

We have analyzed comparatively the accuracy of five propagation models for indoor environment in order to determine a simple procedure for large scale WLAN planning with inexpensive resources since it uses the RSSI that can easily measured using free test software running on a notebook with an 802.11a/b/g card adapter. We have verified that the one-slope and dual-slope models have presented a better agreement than the partition model, which has its parameters pre-determined. For the models that consider the wall attenuation in an explicit way, the average walls model has presented more accurate results in relation to the COST 231 model.

We conclude that the average walls model is a practical and fast procedure for coverage estimation. The standard deviation of error between measured and predicted values are in according to the shadowing standard deviation (typically between 5 and 12 dB).

A similar comparison procedure applied in others *UFRGS's laboratories* have confirmed that the average walls model allows better prediction results among the five path loss models analyzed in this contribution, as shown in Fig 10.

In summary, the results shown in Figures 9 and 10 indicate that this model, that can be parameterized using few measurements, can be expanded through the site with a good accuracy. Currently, for the ongoing UFRGS project, the average walls model has been used for planning WLANs employed for distance learning in low income communities.

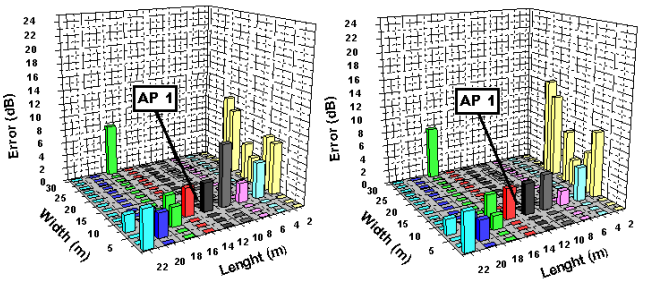

(a) Average walls model for AP1. (b) Dual Slope model for AP1.

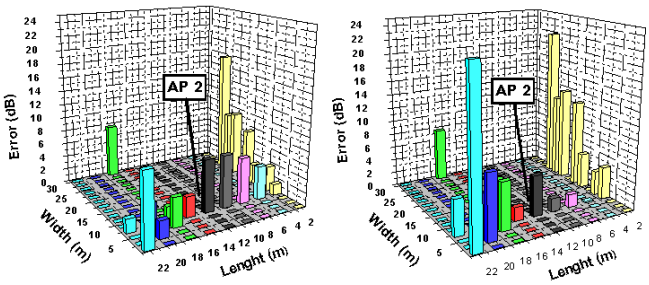

(a) Average walls model for AP2. (b) Dual Slope model for AP2.

Fig. 10 – Errors between received power between estimation and site survey measurement*: supplementary results* **obtained at a different environment** *in relation to the data shown in Fig. 9.*

References

[1] S. Zváinovec, M Válek, P. Pechac, "Results of Indoor Propagation Measurement Campaign for WLAN Systems Operating in 2.4 GHz ISM Band", in *Proc. Antennas and Propagation, 2003. (ICAP 2003). Twelfth International Conference*, 2003, page(s):63 - 66 vol.1.

[2] F. Capulli, C. Monti, M. Vari, F. Mazzenga, "Path Loss Models for IEEE 802.11a Wireless Local Area Networks", *in Proc. Wireless Communication Systems, 2006. ISWCS '06.* , 2006, page(s):621 – 624.

[3] K. Pahlavan and A. H. Levesque*, Wireless Information Networks 2th ed.,* Ed. Wiley, Chichester, England, 2005.

[4] E. Tanghe, W. Joseph, L. Verloock, L. Martens, H. Capoen, K. V. Herwegen, T. Buysschaert, "Range of an IEEE 802.11b/g system in industrial environments based on site survey measurements and propagation models", in *Proc. Antennas and Propagation Society International Symposium*, 2008.

[5] T. S. Rappaport, *Wireless Communications – Principles & Practice*, 2nd ed., Prentice Hall Inc, 1996.

[6] D. Akerberg, "Properties of a TDMA Pico Cellular Office Communication System", in *Proc. Vehicular Technology Conference, 1989 IEEE 39th*, 1989.

[7] COST 231, *Digital Mobile Radio Towards Future Generations Systems,* Final Report – European Comission, 1999.

[8] A. Borrelli, C. Monti, M. Vari, F. Mazzenga, "Channel Models for IEEE 802.11b Indoor System Design", in *Proc. Communications, 2004 IEEE International Conference*, 2004, page(s):3701 - 3705 Vol.6.

[9] J. Lloret, J. J. López, C. Turró and S. Flores, "A fast design model for indoor radio coverage in the 2.4 GHz wireless LAN"*, in Proc Wireless Communication Systems,* 2004.

[10] R. P. F. Hoefel, "IEEE WLANS: 802.11, 802.11e MAC AND 802.11a, 802.11b, 802.11g PHY cross layer link budget model for cell coverage estimation ", in *Proc,Electrical and Computer Engineering, 2008. CCECE 2008. Canadian Conference*, 2008.